Hazardous Bismarck Brown Dye Adsorption on Graphene Oxide and Its Chitosan and Ethylenediaminetetraacetic Acid Derivatives

Alaa A. Mizhir[1], Hadi S. Al-Lami[2,*], Ali A. Abdulwahid[2]

1. Department of Applied Marine Science, The Faculty of Marine Science, University of Basrah, Basrah, Iraq
2. Department of Chemistry, College of Science, University of Basrah, Basrah, Iraq

*Corresponding author E-mail: hadi.abbas@uobasrah.edu.iq

Doi:10.29072/basjs.20220102

ARTICLE INFO

Keywords

Adsorption isotherm, Bismarck Brown, Graphene Oxide; Chitosan, Pseudo-second-order model.

ABSTRACT

Polymeric adsorbents are developed for removal toxic Bismarck Brown (BB) dye. Hummer's method was used to prepare graphene oxide (GO) from graphite with minor alterations. The other two derivatives were made by grafting GO with Chitosan (GO/CS) and ethylenediaminetetraacetic acid (GO/CS/EDTA). Fourier transform infrared spectroscopy (FTIR) was used to analyze their chemical structure. Batch studies were carried out to investigate the adsorption systems of GO and its derivatives against the toxic BB dye, and they showed a good reaction to the adsorption from their aqueous solutions. The effect of pH value on the adsorption systems was investigated and found pH values depending on the type of the adsorbents. It was found that pH 3.0 and 5.0 were the best for the adsorption of BB dye onto GO, GO/CS, and GO/CS/EDTA, with an agitation time of up to 45 min. Adsorption isotherms were determined using Langmuir and Freundlich. The Langmuir model was found to be more appropriate for the experimental results of the adsorption of BB dye on the prepared adsorbents. According to kinetic studies, the pseudo-second-order model fits the experimental data the best. According to the thermodynamic characteristics determined, the adsorption process was spontaneous and endothermic.

Received 7 Mar 2022; Received in revised form 25 Mar 2022; Accepted 16 Apr 2022, Published 30 Apr 2022

1. Introduction

Water pollution is one of the most serious threats to humanity, and it is a hot area of research around the world [1]. It is due to growing industrialization. Due to their non-biodegradable nature, organic dyes, which are pollutant effluents emitted from numerous food and textile sectors, are one of the most significant sources of environmental pollution [2]. Textile manufacturing leaks a significant amount of synthetic organic dyes into rivers and other water sources, polluting the water, preventing sunlight penetration, increasing oxidative stress, and ultimately degrading water quality [3]. Most synthetic dyes, which have a complicated structure with azo groups, induce severe toxicity when absorbed through dye-contaminated water, eventually leading to malignancies in many regions of the human body [4]. As a result, dye removal from wastewater is critical for environmental safety. For the elimination of dyestuffs, various approaches have been documented in the literature, including photocatalysis and adsorption [5]. Flocculation, ultrafiltration, reverse osmosis, precipitation, and other technologies have been developed to remove dye from wastewater. These procedures are costly and do not entirely remove the color, resulting in additional contamination issues [6]. The removal of dye from the environment has become more difficult because of these disadvantages. Researchers continue to choose adsorption because of its straightforward approach, high efficiency, ease of recovery, and adaptability. Furthermore, the adsorbent can be reused several times, and the harmful compounds created during degradation can be avoided [7]. Because of the abundance of oxygen-containing functional groups on the two-dimensional (2D) large surface, such as hydroxyl, carboxyl, and epoxy groups, graphene oxide (GO), an oxidized derivative of graphene, has excellent adsorbent performance for heavy metals, dyes, and pharmaceutical antibiotics [8].

These oxygen-containing functional groups cannot only complicate contaminants in wastewater, but they can also serve as reactive sites for chemical reactions that can be used to functionalize graphene oxide [9]. By using a chemical procedure, a large number of molecules, particularly tiny functional organic molecules, can be grafted onto the surface of graphene oxide [10]. The use of polymers with numerous carboxylic groups, such as poly (acrylic acid) and other analog polymers, to functionalize GO composites has not been described [11]. These polymers have a strong affinity for most positively charged organic contaminants and the ability to promote water dispersibility.

Numerous studies have recently been conducted to investigate the environmental applications of GO and GO-based composite adsorbents, and these composite materials have demonstrated exceptional adsorption capacities against a variety of hazardous chemicals in an aqueous solution [12]. We present a method for preparing a new type of adsorbent based on natural and inexpensive chitosan polymers, namely graphene oxide-g-Chitosan (GO-g-CS) and graphene oxide-g-Chitosan-g-ethylenediaminetetraacetic acid (GO/CS/EDTA), for the removal of Bismarck Brown BB dyes from aqueous solutions. The impact of experimental variables like pH and temperature was studied. Langmuir and Freundlich's isotherms were used to describe the adsorption mechanisms.

2. Experimental

2.1 Materials

Natural graphite with a purity of 99.99% was purchased from Hopkin & Williams Co. Ltd. and was used to prepare Graphene Oxide (GO). Merck & Co. supplied chitosan (80 mesh) with a degree of deacetylation (75%–85%). Concentrated sulfuric acid (H_2SO_4), sodium nitrate and sodium chlorate ($NaNO_3$ and $NaClO_4$), potassium permanganate ($KMnO_4$), hydrogen peroxide (H_2O_2, 30%), hydrochloric acid (HCl, 36%), sodium hydroxide (NaOH), N, N′-dicyclohexylcarbodiimide (DCC), and acetic acid were provided by Sigma-Aldrich Company.

2.2 Instruments

To investigate the chemical structures, Fourier transforms infrared FTIR spectra of compounds were analyzed using an FTIR-8101M Shimadzu spectrometer with a KBr pellet in the 400–4000 cm-1 range. The concentration of BB dye was measured in a quartz cell of 1 cm length at λ_{max} = 457 nm using a Sentry 20 UV-Visible spectrophotometer model T180.

2.3 Synthesis of Graphene Oxide (GO)

A modified Hummers' method [13] was used to make GO. Under a cold bath, 2.0 g of graphite powder and 1.0 g of $NaNO_3$ were dissolved in 46.0 mL of H_2SO_4 (98%). Following 15 minutes of stirring, 6.0 g of $KMnO_4$ was gradually added to the suspension, stirring as slowly as possible to keep the temperature below 20°C. The suspension was agitated for 2 hours and kept at 35°C for 30 minutes. The temperature was quickly raised when 100.0 mL of deionized water was added to the suspension, and the temperature should be kept below 98°C. The suspension was

then diluted to 280.0 mL with warm deionized water after 15 minutes. 20.0 mL of H_2O_2 (30%) was added to the suspension, which changed the hue to bright yellow. The suspension was filtered and washed with a warm aqueous solution of 5% HCl and deionized water until no sulfates were found and the pH of the filtrate was adjusted to 7.0. The graphene oxide GO was dried at 50°C in a vacuum.

2.4. Synthesis of Graphene Oxide-Chitosan Composite (GO/CS)

With slight adjustments, the GO/CS was prepared according to the literature [14]. Ultrasonication was used to disperse 0.5 g of GO in 50.0 mL of distilled water for 3 hours. To activate the carboxyl groups of GO, a solution of 0.05 M (0.0478 g) N,N-di-cyclohexyl carbodiimide (DCC) was added with continuous stirring to the GO dispersion for 2 hours [15]. A 2% NaOH solution was used to raise the pH to 7.0. The activated GO solution with 5.0 g of Chitosan CS was then ultrasonically dispersed in 50.0 mL of distilled water and 50 mL of 10% acetic acid for 20 minutes. After that, the mixed solutions were agitated for another 3 hours at 60°C. After filtration, the precipitate was washed with a 10% NaOH solution and deionized water until the pH was around 7.0. In a vacuum oven, the GO/CS product was dried. The preparation route of the GO/CS derivative is shown in Scheme 1.

2.5. Synthesis of GOCS–Ethylenediaminetetraacetic Acid Composite (GO/CS/EDTA)

The functionalization of GO/CS by EDTA was achieved by modifying a previously published approach [16]. To make a GO/CS dispersion, 0.5 g of GO/CS was evenly dispersed in 20.0 mL of 10% acetic acid aqueous solution for 2 hours, and 6.0 g of EDTA was evenly dispersed in 100.0 mL of methanol for 2 hours. The mechanical rumbling was used to combine the GO/CS and EDTA dispersions, which were then left to react at room temperature for 24 hours. The GO/CS/EDTA product was filtered and washed twice with deionized water before being dried in a vacuum oven at 50 °C and ground into a fine powder. Scheme 2 suggests the preparation pathway of the GO/CS/EDTA derivative.

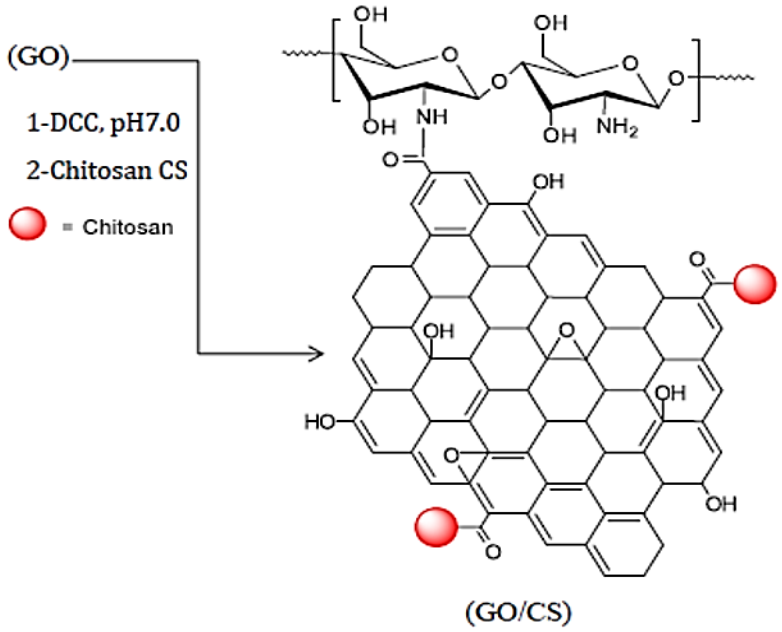

Scheme 1: The preparation route for the GO/CS adsorbent.

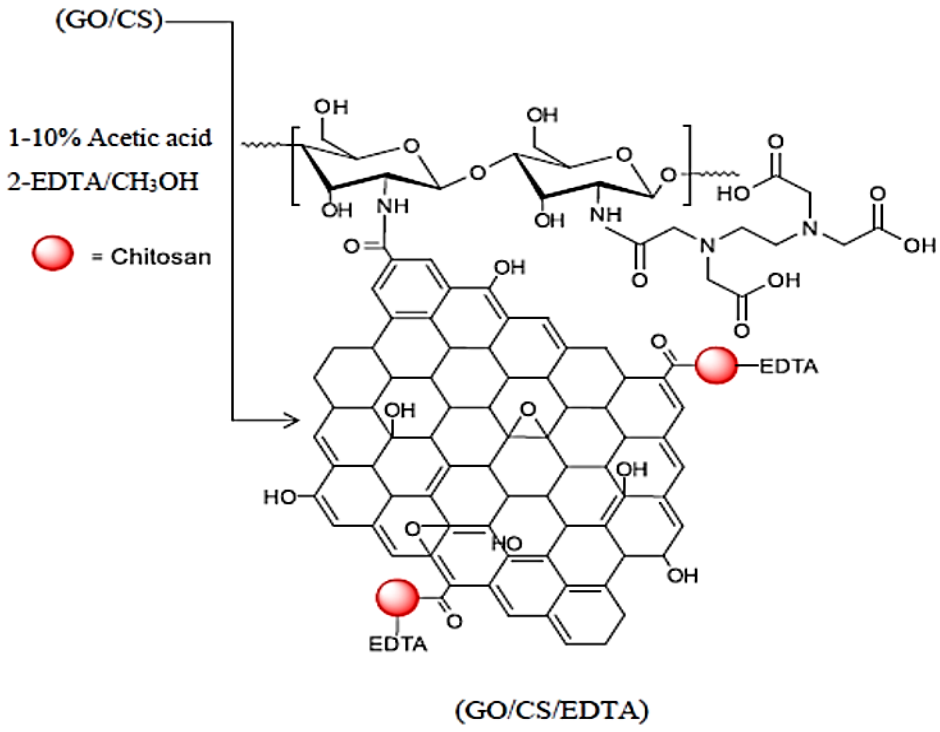

Scheme 2: The preparation route for the GO/CS/EDTA adsorbent.

2.6 Preparation of Aqueous Dye Solution

Bismarck Brown (BB) (FW = 419.31) was used without any purification in this study, and its chemical structure is shown in Fig. 1. A stock solution of the BB dye at 1000.0 mg/L was prepared for the adsorption experiments, and then the required concentrations were provided with the dilution by using ultra-deionized water.

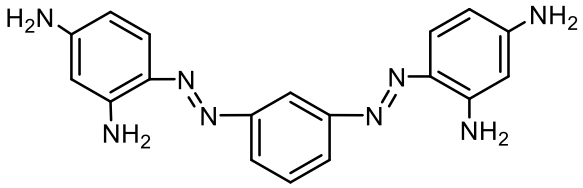

Figure 1: Chemical structure of the Bismarck Brown BB [17].

2.7 Batch Adsorption Experiments

The adsorption experiments were carried out by contacting a 0.025 g fixed weight of adsorbents with a 0.1L of BB dye solution with a chosen initial concentration on each adsorbent, shaking the solutions at 200.0 rpm for 24 hours at 27°C, and filtering the resulting suspensions. A UV-Visible Spectrophotometer set to lambda max 457 nm was used to estimate the equilibrium concentration. The amount of BB dye on the produced adsorbents was determined from the difference in dye concentration in the aqueous phase before and after adsorption using equation 1[18]:

$$q_e = \frac{(C_o - C_e)\,V}{m} \quad \ldots\ldots \qquad 1$$

Where C_o and C_e (mg/L) are the initial and equilibrium concentrations of dye in the solution, V (L) is the volume of dyes solution, m (g) is the mass of the used adsorbents in the experiment, and q_e (mg/g) is the amount of adsorbed dye per gram of adsorbents GO, GO/CS, and GO/CS/EDTA.

2.8 Optimization of Adsorption Experiments

2.8.1 The initial concentration of BB dye

To perform the optimal initial concentration of BB dye, different concentrations are prepared; 100, 200, 300, 400, 500, and 600 mg/L. BB dye was recorded at 400.0 mg/L as an optimum initial concentration for the prepared adsorbents, i.e., GO, GO/CS, and GO/CS/EDTA.

2.8.2 The effect of pH

At 400.0 mg/L as an initial concentration of adsorbents GO, GO/CS, and GO/CS/EDTA, and 0.025 g as a fixed weight of prepared adsorbents with 0.1L of BB solutions, the influence of pH on BB dye adsorption was investigated for 24 hours at 27°C. The pH of the BB dye solution was adjusted by 0.10 M of hydrochloric acid or sodium hydroxide solution. After filtration, the adsorbents were removed from the solution, and the equilibrium concentration of the remaining BB dye was estimated at λmax 457 nm using a UV-Visible Spectrophotometer.

2.9 Determination of contact time for BB Dye

To determine the equilibrium time of the adsorption study, a volume of 0.1L was added to a fixed 0.025 g as a known amount of prepared adsorbents. All solutions were shaken at 200.0 rpm for 1, 3, 9, 12, 15, 30, 45, 60, 75, and 90 min at room temperature. Adsorbents were then separated from the solution by filtration and the equilibrium concentration of residual BB dye was determined using a UV-Visible Spectrophotometer at λmax 457 nm and optimum pH 3.0 for GO and GO/CS, and 5.0 for GO/CS/EDTA.

2.10 Adsorption Isotherms

At equilibrium, the adsorption isotherm depicts the distribution of molecules between solid and liquid phases. The fitting of isotherm data to multiple isotherm models is an important step in determining the best appropriate model for describing the adsorption process [19, 20]. Isotherm data can be described using a variety of isotherm models. The Langmuir and Freundlich isotherm models are used to assess the experimental results in this work. The maximum adsorption that coincides with the saturated monolayer of liquid (adsorbate) molecules on the solid (adsorbent) surface is what the Langmuir model is based on. The linearized form of the Langmuir model is given as follows [21].

$$\frac{C_e}{q_e} = \frac{1}{(q_{max}.K_L)} + \frac{C_e}{q_{max}} \quad \ldots\ldots \qquad 2$$

Where C_e (mg/L) is the CR dye equilibrium concentration; q_{max} (mg/g) is the adsorption capacity required to complete a monolayer on the adsorbent surface; q_e (mg/g) is the amount of adsorbate per unit mass of adsorbent at equilibrium (mg/g), and K_L is a Langmuir constant that relates to the energy of adsorption. The Langmuir equation is valid for monolayer adsorption of the adsorbate onto the surface of the adsorbent, and it assumes that the adsorption sites are restricted and homogeneous. A dimensionless constant separation factor or equilibrium parameter R_L [22] can be used to characterize the key properties of a Langmuir isotherm.

$$R_L = \frac{1}{1 + (K_L.C_e)} \quad \ldots\ldots \qquad 3$$

R_L is indicative of the isotherm shape and predicts whether a sorption system is either favorable ($0 < R_L < 1$), unfavorable ($R_L > 1$), or irreversible ($R_L = 0$) [23]. The Freundlich isotherm is based on a heterogeneous exponentially decaying distribution, which corresponds to the tail section of the heterogeneous adsorbent distribution [24]. The empirical equation for the general Freundlich isotherm is:

$$\ln q_e = \ln K_F + \frac{1}{n} \ln C_e \quad \ldots\ldots \qquad 4$$

Where K_F (L/mg) is a constant for the adsorption or distribution coefficient and represents the amount of dye adsorbed onto adsorbents at equilibrium concentration.

2.11 Kinetic Studies

Kinetics data helps to depict dye uptake rates, which control the residence time of adsorbate at the solid-liquid interface and give helpful information for adsorption process design [25]. Experimental kinetic curves can be assessed using various models [26]. In this study, the appropriateness of pseudo-first-order and pseudo-second-order was tested to interpret the mechanism of BB dye adsorption onto GO, GO/CS, and GO/CS/EDTA. The linear form of the two kinetic model equations can be expressed as [27]:

$$\ln q_{e\_}q_t = \ln q_1 - k_1 t \quad \ldots\ldots \qquad 5$$

$$\frac{t}{q_t}=\frac{1}{K_2.q_2^2}+\frac{t}{q_2} \quad \ldots\ldots \qquad 6$$

Where q_t and $q_{(1+2)}$ are the dye adsorbed amounts at time t and equilibrium, respectively; K_1 is the adsorption rate constant of the pseudo-first-order model and K_2 is the adsorption rate constant of the pseudo-second-order model.

2.12. Adsorption Thermodynamics

Thermodynamic parameters can be determined from the thermodynamic equilibrium constant, K_L, or the thermodynamic distribution coefficient [28], whereas K_L is equal to:

$$K_L=\frac{C_a}{C_e} \quad \ldots\ldots \qquad 7$$

The equilibrium dye concentrations on the adsorbents (mg/g) and in the solution (mg/L) are Ca and Ce, respectively. The results of thermodynamic studies make it possible to understand the feasibility of the adsorption process and obtain useful data about fundamental adsorption parameters such as the change of standard enthalpy (ΔH°), change of standard entropy (ΔS°), and change of standard free energy (ΔG°), which can be calculated using Equations (8 and 9) [29]:

$$\ln K_L=\frac{\Delta S^\circ}{R}-\frac{\Delta H^\circ}{RT} \quad \ldots\ldots \qquad 8$$

$$\Delta G^\circ = \Delta H^\circ - T\Delta S^\circ \quad \ldots\ldots \qquad 9$$

Plotting lnKL vs 1/T yields ΔH° (kJ/mol) from the slope and ΔS° (JK^{-1}/mol) from the intercept, where R is the universal gas constant (8.314 J/mol K) and T (K) is the absolute temperature. While the Helmholtz relation equation was used to calculate the standard Gibbs free energy values (ΔG°, kJ/mol) for each temperature utilized in adsorption procedures (Equation 9). The adsorption process' activation energy, Ea (kJ/mol), represents the minimum energy that reactants have for the reaction to proceed, and it was derived using the Arrhenius equation, as indicated by the following relationship [30]:

$$\ln K = \ln A - \frac{E_a}{RT} \quad \ldots\ldots \qquad 10$$

Where k (g mg^{-1} min^{-1}) is the rate constant calculated using the pseudo-second-order kinetic model for the three adsorbents in an adsorption system with BB dye, and A is the Arrhenius factor. When you plot ln k against 1/T, a straight line with a slope of –Ea/R was obtained.

3. Results and Discussion

3.1 FTIR Characterization of Adsorbents

FTIR spectroscopy was used to investigate the existence of extra-functional groups on the modified graphene oxide GO surface. The spectrum of layer graphite powder is largely featureless [13, 31], whereas GO (Fig. 2) has significant bands at 3367 cm^{-1}, which corresponds to hydroxyl stretching vibration, and 1728 cm^{-1}, which corresponds to carbonyl stretching vibration. Aromatic C=C stretching vibrations were blamed for the peak at 1620 cm^{-1}. The FTIR spectra of graphene oxide and graphite were significantly different, with a large number of oxygen-containing functional groups present in the basal and edge planes of the graphene oxide sheet [30], and the differences were proportionate to those previously described [31], indicating that the graphene oxide was successfully prepared. The IR spectrum of the GO/CS composite shows a combination of characteristic peaks of Chitosan CS and Graphene Oxide GO (Fig.3). Therefore, the results implied that interactions existed between them [32]. The stretching vibration bands of the C–H at 2928, and 2852 cm^{-1} come from the $–CH_3$ of Chitosan, indicating that GO was successfully grafted onto Chitosan. Furthermore, there are some distinct absorbance bands at 3326, 1642, and 1577 cm^{-1} that correspond to the N–H stretching vibration, C=O stretching of –NHCO–, and N–H bends of $–NH_2$ [33]. The interaction between GO and CS may result in a new peak at 1453 cm^{-1} due to C-H bending and a shift of the characteristic peak of O–H from around 3367 to 3326 cm^{-1} [34, 35].

The FTIR spectrum of the GO/CS/EDTA derivative (Fig. 4) indicates some exciting alterations. After grafting EDTA to GO/CS, the intensity of the N–H absorption peak at 3326 cm^{-1} was considerably reduced. The N-H stretching vibrations above 3000 cm^{-1} were weakened, and the peak of N-H bending vibrations at 1577 cm^{-1} has vanished. Due to the CO stretching vibration of new COO groups from EDTA [36], a new strong peak at 1317 cm^{-1} appears. Furthermore, the C=O stretching vibration peak in GO/CS shifts from 1642 cm^{-1} to 1694 cm^{-1} in GO/CS/EDTA, implying that interactions exist between GO/CS and EDTA.

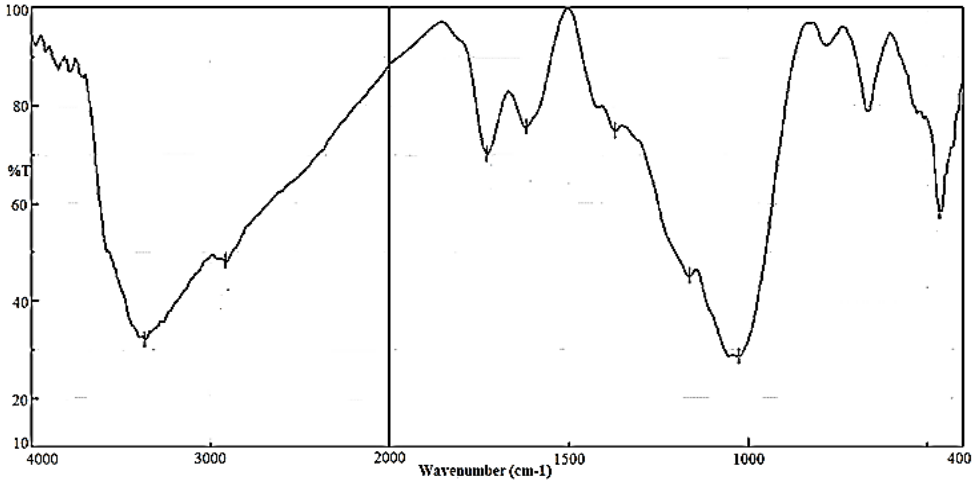

Figure 2: FTIR spectrum of the GO adsorbent.

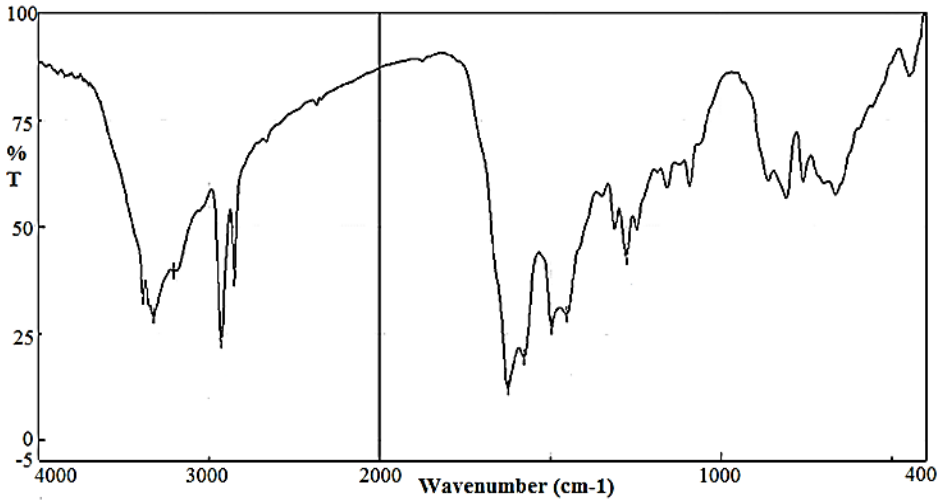

Figure 3: FTIR spectrum of the GO/CS adsorbent.

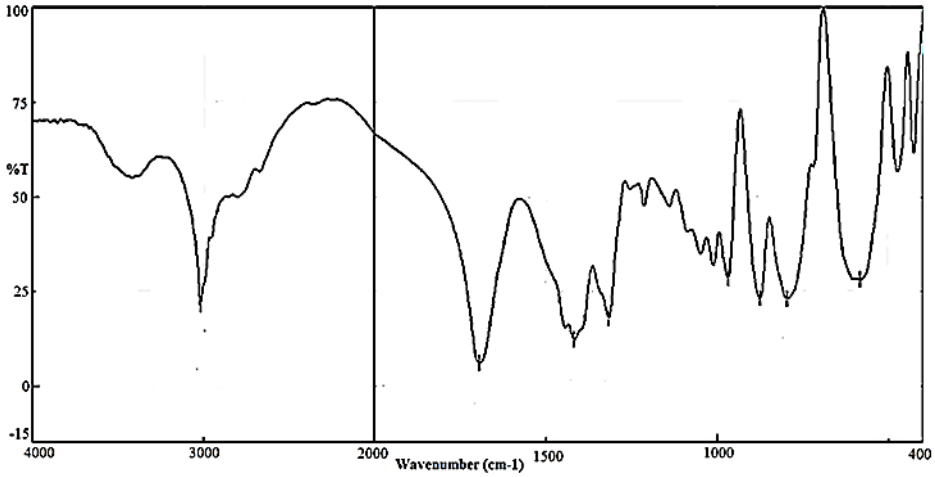

Figure 4: FTIR spectrum of the GO/CS/EDTA adsorbent.

3.2 Adsorption of BB dyes onto GO and GO

A batch system was employed in adsorption experiments of BB dyes onto prepared adsorbents GO, GO/CS, and GO/CS/EDTA at optimum pH, contact time, and temperature.

3.2.1 Effect of pH

The pH of the dye solution plays a significant role in the whole adsorption experiment, particularly in the adsorption capacity. The pH solution can affect the surface charge of the adsorbent and the degree of ionization of different pollutants [37]. The effect of pH on the adsorption capacities of prepared adsorbents was studied at an optimum initial concentration of BB dye. Fig. 5 illustrates the pH influence of the adsorption capacities (q_{max}) at 27°C for BB dye adsorption onto GO, GO/CS, and GO/CS/EDTA. The pH of BB dye solutions was then adjusted individually to values within the range of 3.0–12.0. According to the results obtained, the optimal pH levels vary depending on the type of adsorbent. The optimum pH for the adsorption of BB dye onto GO, GO/CS, and GO/CS/EDTA was found to be 3.0, 3.0, and 5.0, respectively.

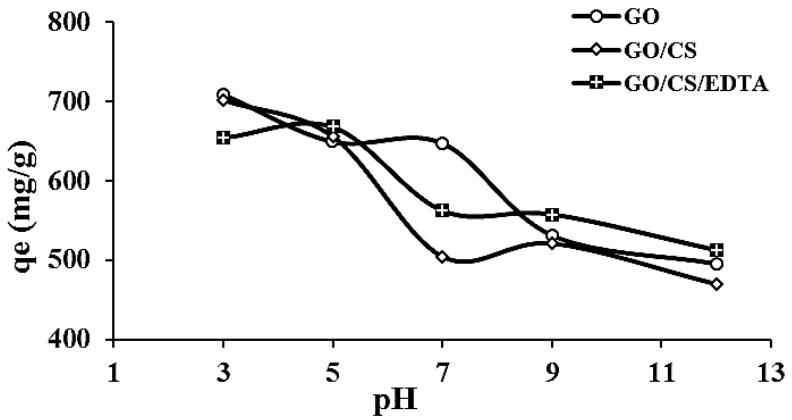

Figure 5: Effect of pH on the adsorption of Bismarck Brown BB onto Adsorbents at 27°C.

3.2.2 The influence of agitation time and temperature on BB adsorption

Agitation time is the amount of time that passes until the adsorption experiment research reaches equilibrium [38]. As a result, the contact time between the adsorbate and the adsorbent is critical in the adsorption process, and the time required to reach equilibrium is crucial in predicting the performance and practicality of an adsorbent for a given procedure [39]. Figures 6–8 illustrated the influence of agitation duration on the adsorption of BB dye onto the prepared

adsorbents GO, GO/CS, and GO/CS/EDTA, respectively, at the initial concertation of each adsorbent and optimal pH in three distinct temperatures ranges of 27, 40, and 60 °C. All the figures illustrate a rapid increase from 1–45 min., and then the equilibrium is reached within contact time (45–75 min.) for GO, GO/CS, and GO/CS/EDTA. The adsorption capacity for all adsorbents GO, GO/CS and GO/CS/EDTA increased as the temperature rose from 27 to 60°C, and this tendency for adsorption capacities is expected. Thus, the optimum agitation times for all further experiments were chosen as 45 min. for the adsorption of BB dye onto GO, GO/CS, and GO/CS/EDTA adsorbents.

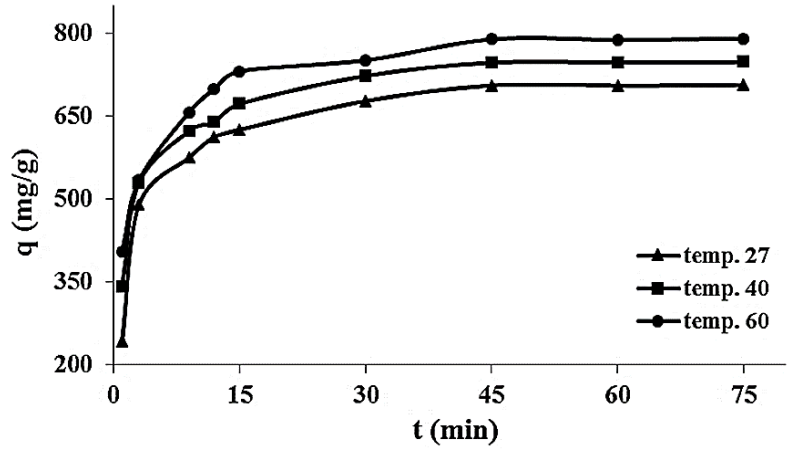

Figure 6: Agitation time effect of the BB dye adsorption onto GO at different temperatures.

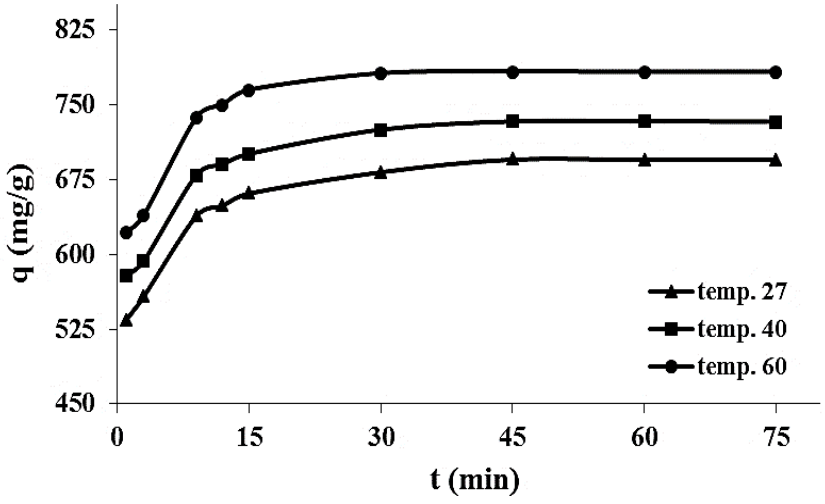

Figure 7: Agitation time effect of the BB dye adsorption onto GO/CS at different temperatures.

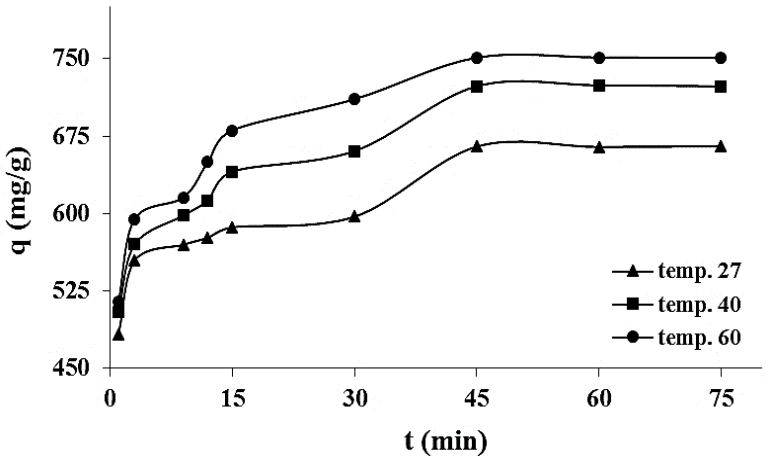

Figure 8: Agitation time effect of the BB dye adsorption onto GO/CS/EDTA at different temperatures.

3.3 Langmuir and Freundlich Adsorption Isotherms

Fitting the data into different isotherm models is an essential step in finding the most reasonable model that can be used to explain the adsorption process [39]. The Langmuir model depends upon the maximum adsorption coinciding with the saturated monolayer of adsorbate molecules on the adsorbent surface. The maximum adsorption (q_{max}) was calculated using the Langmuir isotherm results, and they were (833.94, 920.74, and 863.8 mg/g) for GO, GO/CS, and GO/CS/EDTA, respectively, and for the adsorption of BB dye for the same adsorbents order mentioned previously. Again, these results proved the preference for prepared GO derivatives over GO. When plotting Ce/qe versus Ce, the slope of a plot is equal to ($1/q_{max}$) and the intercept is equal to ($1/q_{max}$. KL). Fig. 9 shows the plots of the Langmuir adsorption isotherm of BB dye adsorbed onto GO, GOCS, and GO/CS/EDTA, and Table 1 displays the qmax, kL, RL, and the correlation coefficient R^2 results for the Langmuir isotherms for the adsorption of the BB dye by the prepared adsorbents.

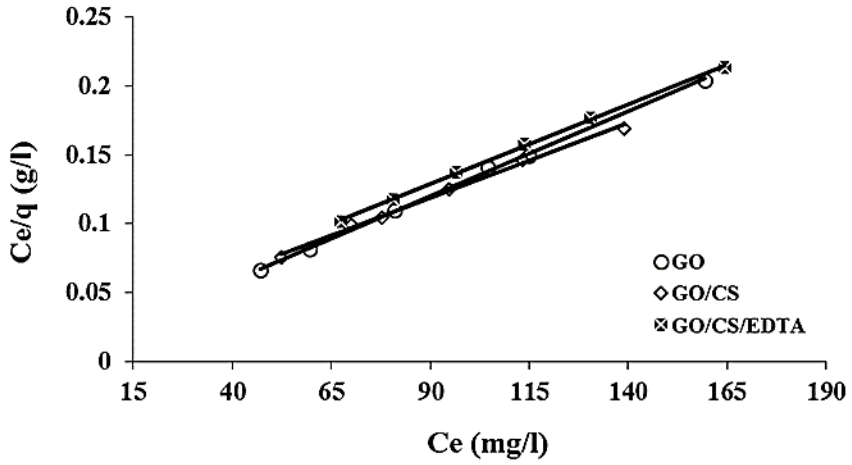

Figure 9: Langmuir adsorption isotherm of BB dye onto different adsorbents at 27°C.

Table 1: Langmuir and Freundlich isotherm parameters for BB dye adsorption onto prepared adsorbents at 27°C.

Adsorbent	Langmuir Parameters				Freundlich Parameters		
	q_{max}	k_L	R_L	R^2	k_F	1/n	R^2
GO	833.33	0.1263	0.0994	0.9988	527.158	0.7720	0.9004
GO/CS	920.74	0.0531	0.0449	0.9958	353.966	0.1682	0.9492
GO/CS/EDTA	863.88	0.0491	0.0483	0.9958	337.782	0.1612	0.9926

The obtained correlation coefficients R^2 for the Langmuir (as shown in Table 1) are $0.9988 \geq R^2 \geq 0.9958$ for BB dye. This describes the participation of the chemisorption mechanism in the adsorption process of dyes on the prepared adsorbents. In addition, to determine whether the adsorption process is favorable or unfavorable for the Langmuir isotherm model, the values of constant separation factor R_L, defined in equation (3), are all between one and zero ($0.0483 \leq R_L \leq 0.0994$), implying the presence of favorable conditions for the adsorption process of the prepared adsorbents by BB dye. Besides that, the R_L values of the GO/CS and GO/CS/EDTA adsorbents shown in Table 1 are lower than R_L of graphene oxide, which reflects the higher affinity of the latter adsorbents toward the BB dye. This is accompanied by the higher q_{max} of the

GO/CS and GO/CS/EDTA than GO itself; this indicates the ability and high efficiency of these adsorbents to adsorb BB dye from its aqueous solutions by the adsorption process. The other isotherm model studied were the Freundlich isotherm model, which is based on a heterogeneous exponentially decaying distribution. The general Freundlich isotherm empirical equation is given by equation 4. Fig. 10 shows the plots of the Freundlich adsorption isotherms of BB dye adsorbed onto GO, GO/CS, and GO/CS/EDTA, and Table 1 lists k_F, 1/n, and the correlation coefficient R^2 is determined from the linear plot of ln qe versus ln Ce.

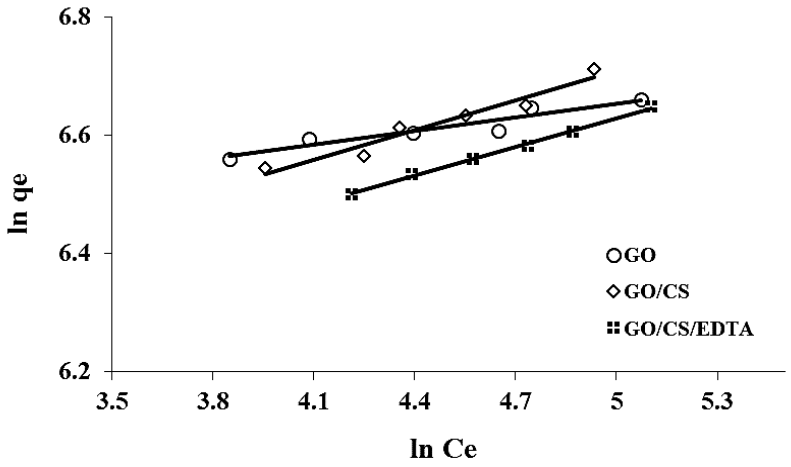

Figure 10: Freundlich adsorption isotherm of BB dye onto various adsorbents at 27°C.

The obtained R^2 for the Langmuir was more than that of the Freundlich isotherm equation, $0.9926 \geq R^2 \geq 0.9004$. This also describes the participation of the chemisorption mechanism in the adsorption process on the prepared adsorbents. In addition, the results showed that k_F ranged from 337.785 to 527.158 $L.mg^{-1}$ while 1/n values ranged from 0.1612 to 0.7020, as shown in Table 1, which reflects the strength and practicality of the adsorption process. The 1/n values are less than one, suggesting favorable adsorption of BB dye on adsorbents.

3.4 Kinetic Studies on Adsorption

The adsorption mechanism of BB dye onto GO, GO/CS, and GO/CS/EDTA was investigated using two kinetic models at temperatures of 27, 40, and 60 °C. The first model was the pseudo-first-order, equation (5). Plotting of $1/q_t$ versus 1/t gives the rate constants K_1 and R^2 determined from Figs. 11-13 and tabulated in Table 2.

The second kinetic model was pseudo-second-order as given in equation 6. Values of q_2 and K_2 were calculated from the plot of t/q_t versus t from the slope and intercept of Figs. 14-16 and are listed in Table 2 for the adsorption of BB dye onto the same adsorbents at different temperatures (27, 40, and 60°C). The R^2 values from two kinetics models for BB dye adsorption are ≤ 0.9960 and ≤ 1.000 for the pseudo-first-order and pseudo-second-order, respectively. Furthermore, the calculated q matches highly effectively with the experimental data. This suggests that the kinetic modeling of the temperature effect is more likely to fit the models of the pseudo-second-order adsorption [40].

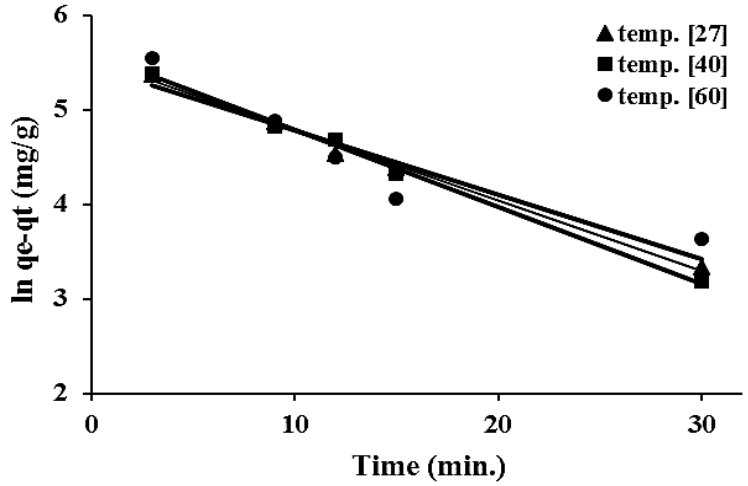

Figure 11: Pseudo-First-Order plot for the adsorption of BB dye onto GO at 27°C, 40°C, and 60°C.

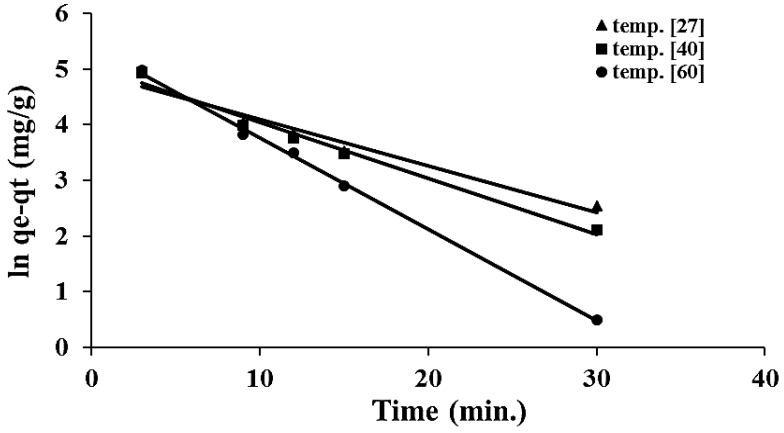

Figure 12: Pseudo-First-Order plot for the adsorption of BB dye onto GO/CS at 27°C, 40°C, and 60°C.

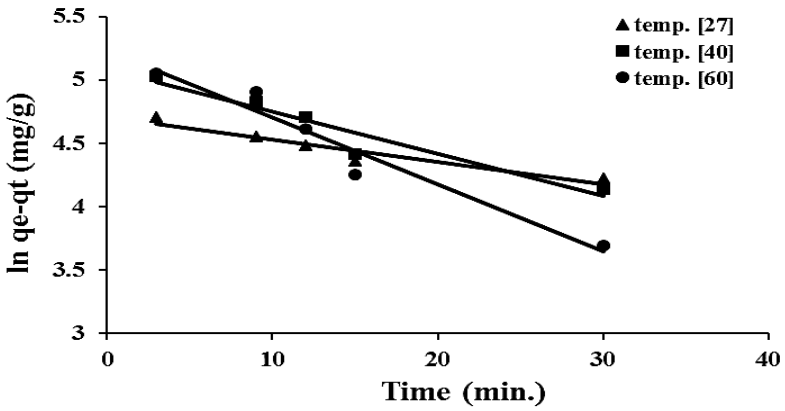

Figure 13: Pseudo-First-Order plot for the adsorption of BB dye onto GO/CS/EDTA at 27°C, 40°C, and 60°C.

Table 2: Kinetic parameters for adsorption of CR and BB dyes onto prepared adsorbents at different temperatures

Adsorbent	Temp. (°C)	Pseudo-first-order			Pseudo-second-order		
		K_1	q_1	R_1^2	K_2	q_2	R_2^2
GO	27	0.0745	251.36	0.9922	0.00065	735.17	0.9992
	40	0.0812	251.36	0.9960	0.00063	778.38	0.9993
	60	0.0679	235.61	0.8633	0.00060	816.78	0.9993
GO/CS	27	0.0836	137.93	0.9583	0.00140	708.66	0.9999
	40	0.1007	154.90	0.9811	0.00141	746.93	1.0000
	60	0.1645	222.85	0.9982	0.00144	796.71	1.0000
GO/CS/EDTA	27	0.0176	110.71	0.9180	0.00090	669.30	0.9992
	40	0.0335	161.59	0.9256	0.00073	737.14	0.9959
	60	0.0527	186.97	0.9495	0.00070	771.71	0.9982

K_1: (min^{-1}), q: (mg/g), K_2: (g mg^{-1} min^{-1})

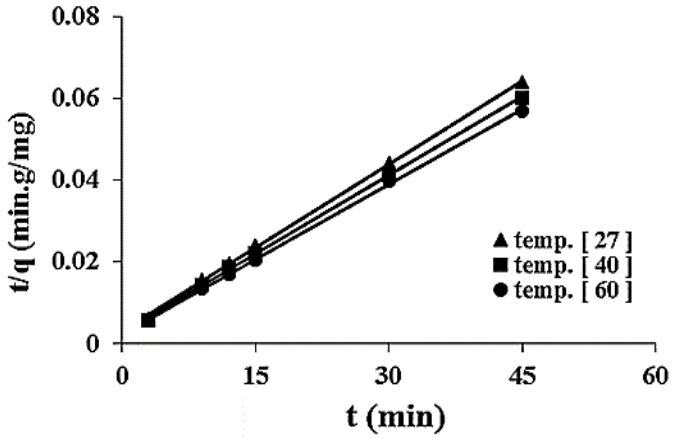

Figure 14: Pseudo-Second-Order plot for the adsorption of BB dye onto GO at 27°C, 40°C, and 60°C.

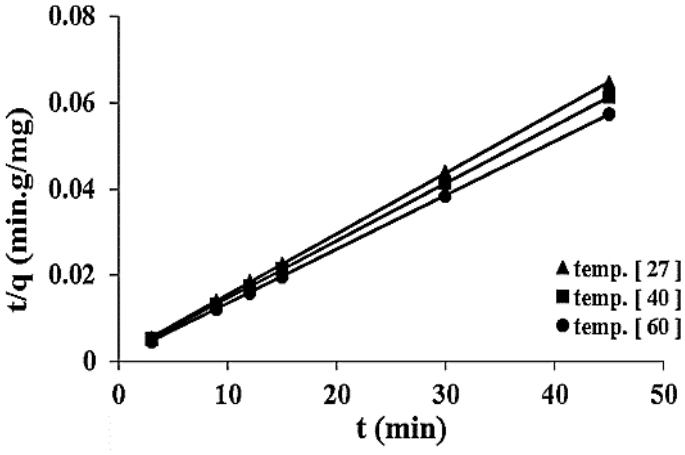

Figure 15**:** Pseudo-Second-Order plot for the adsorption of BB dye onto GO/CS at 27°C, 40°C, and 60°C.

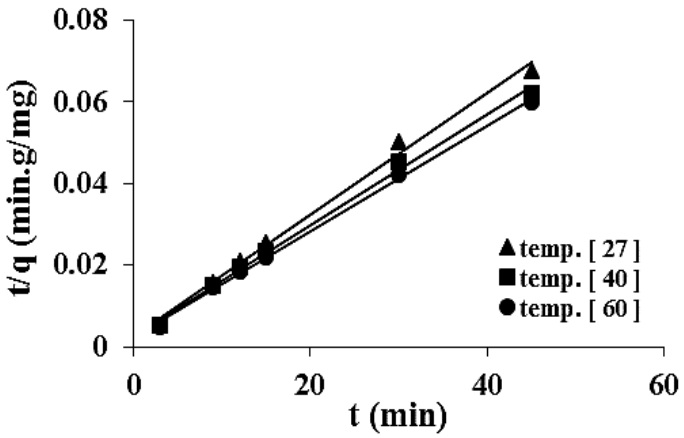

Figure 16: Pseudo-Second-Order plot for the adsorption of BB dye onto GO/CS/EDTA at 27°C, 40°C, and 60°C.

3.5 Thermodynamic Study

The fundamentals of adsorption reactions require an understanding of thermodynamic functions such as the change of standard enthalpy ΔH°, the change of standard entropy ΔS°, the change of standard free energy ΔG°, and the activation energy Ea [41]. The thermodynamic adsorption study was carried out at three different temperatures; 300.15, 313.15, and 333.15 K. Figs. 17-19 show the results of plotting ln K_L versus 1/T from equation 8. The ΔH° (kJ/mol) from the slope and ΔS° (J/mol/K) are determined from the intercept for the adsorption of BB dye onto the prepared adsorbents GO, GO/CS, and GO/CS/EDTA, respectively, and the free energy changes are calculated using equation 9 and its values are shown in Table 3. The negative values of ΔG° indicate that the adsorption process is spontaneous, reflecting the affinity of adsorbents towards BB dye [42]. The positive value of ΔH° confirms the endothermic nature of the adsorption. The positive value of ΔS° for the adsorption of the dyes onto the adsorbents explains the increase in the adsorption process randomness and affinity of the adsorbents for BB dye [43]. The low activation energies (E_a < 40 kJ/mol) for all the three adsorbents with BB dye are governed by the physisorption mechanism involving Van der Waals forces between the charged sites of the dyes and the surface of the adsorbents [44]. As a result, the adsorption process gives an impression of chemical and physical behavior, where the adsorption process might be chemisorption as shown previously in the Langmuir isotherm study and physisorption through the thermodynamic study. Therefore, this means that the adsorption process of BB dye onto adsorbents was a physiochemical adsorption approach.

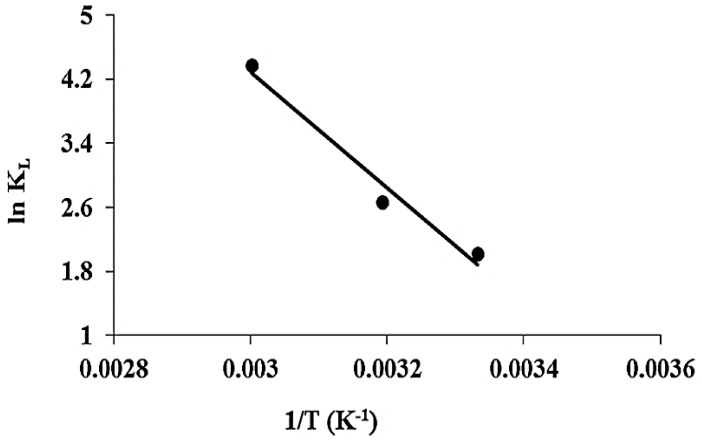

Figure 17: The plot of ln K_L vs. 1/T for estimation of thermodynamic parameters of the BB dye adsorption onto GO.

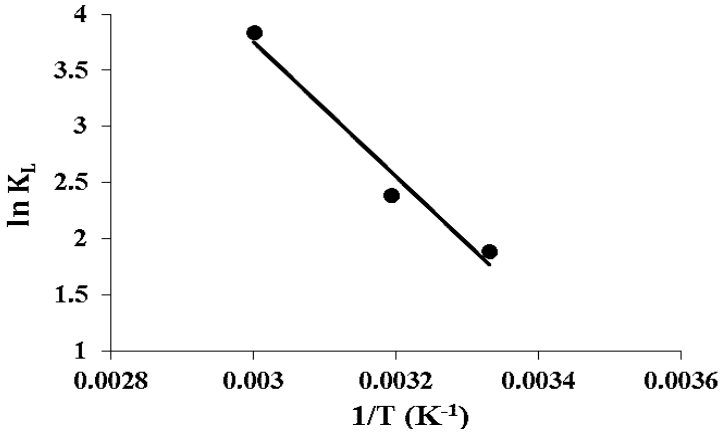

Figure 18: The plot of ln K_L vs. 1/T for estimation of thermodynamic parameters of the BB dye adsorption onto GO/CS.

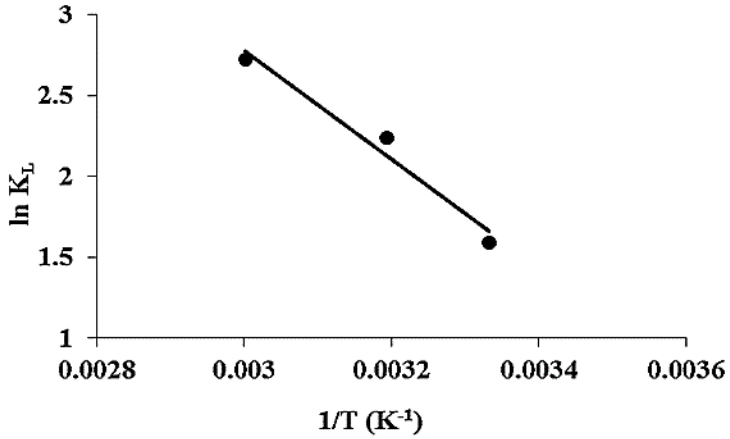

Figure 19: The plot of ln K_L vs. 1/T for estimation of thermodynamic parameters for the BB dye adsorption onto GO/CS/EDTA.

Table 3: Thermodynamic parameters for adsorption of BB dye onto adsorbents at different temperatures.

Adsorbent	Temp.	ΔH°	ΔS°	- ΔG°	Ea
GO	300.15	60.175	216.172	4.709	35.524
	313.15			7.519	
	333.15			11.843	
GO/CS	300.15	49.732	180.439	4.426	0.7255
	313.15			6.771	
	333.15			10.380	
GO/CS/EDTA	300.15	28.063	107.309	4.144	-5.879
	313.15			5.539	
	333.15			7.686	

Temp: (K°), ΔH°, ΔG° & E_a: (kJ/mol), ΔS°: (J K^{-1} mol^{-1})

4. Conclusions

In our study, the modified Hummer method was used to successfully prepare graphene oxide (GO) and its GO/CS and GO/CS/EDTA derivatives, which were characterized using FTIR spectroscopy. They were utilized to remove the harmful Bismarck Brown dye, and they exhibited a good reaction to adsorption from aqueous solutions as well as a pH dependence. According to the findings, the ideal pH levels vary based on the type of adsorbent. The pH (3.0, 3.0, and 5.0) was shown to be the best for adsorption of BB dye onto GO, GO/CS, and GO/CS/EDTA, respectively, and the adsorption process showed a rapid increase with contact duration from (1-45 min.) before reaching equilibrium between (45-75 min.).

As the temperature rose from 27 to 60°C, the adsorption capacity of all adsorbents GO, GO/CS, and GO/CS/EDTA increased, and this trend in adsorption capacities is expected. The maximum adsorption (q_{max}) for GO, GO/CS, and GO/CS/EDTA, respectively, was computed using the Langmuir isotherm results and was (833.3, 920.74, and 863.8 mg/g), proving that produced GO derivatives have a preference for GO. Depending on the R^2 value, the pseudo-

second-order model accurately described the adsorption kinetics for BB dye onto the prepared adsorbents, and the thermodynamic parameters revealed that the adsorption process was spontaneous and endothermic.

References

[1] S. Shahabuddin, R. Khanam, M. Khalid, N.M. Sarih, J.J. Ching, S. Mohamad, R. Saidur, Synthesis of 2D boron nitride doped polyaniline hybrid nanocomposites for photocatalytic degradation of carcinogenic dyes from aqueous solution, Arab. J. Chem., 11 (2018) 1000-1016. https://doi.org/10.1016/j.arabjc.2018.05.004

[2] X. Zhou, P. Zheng, L. Wang, X. Liu, Preparation of sulfonated poly (arylene ether nitrile)-based adsorbent as a highly selective and efficient adsorbent for cationic dyes, Polymers, 11 (2019) 32. https://doi.org/10.3390/polym11010032

[3] B. Fatima, S.I. Siddiqui, R. Ahmed, S.A. Chaudhry, Green synthesis of f-CdWO4 for photocatalytic degradation and adsorptive removal of Bismarck Brown R dye from water, Water Resour. Ind., 22 (2019) 100119. https://doi.org/10.1016/j.wri.2019.100119

[4] S.I. Siddiqui, G. Rathi, S.A. Chaudhry, Acid-washed black cumin seed powder preparation for adsorption of methylene blue dye from aqueous solution: thermodynamic, kinetic and isotherm studies, J. Mol. Liq., 264 (2018) 275-284. https://doi.org/10.1016/j.dib.2018.08.096

[5] B. Sherino, S.N. Abdul Halim, S. Shahabuddin, S. Mohamad, Simultaneous removal of carcinogenic anionic and cationic dyes from environmental water using a new Zn-based metal-organic framework, Sep. Sci. Technol., (2020) 1-14.
https://doi.org/10.1080/01496395.2020.1713815

[6] S.-k. Wu, Y. Pan, N. Wang, T. Lu, W.-j. Dai, Azo dye degradation behavior of AlFeMnTiM (M= Cr, Co, Ni) high-entropy alloys, Int. J. Min. Met. Mater., 26 (2019) 124-132. https://dx.doi.org/10.1007/s12613-019-1716-x

[7] S. Kim, C.M. Park, M. Jang, A. Son, N. Her, M. Yu, S. Snyder, D.-H. Kim, Y. Yoon, Aqueous removal of inorganic and organic contaminants by graphene-based nano adsorbents: A review, Chemosphere, 212 (2018) 1104-1124. https://doi.org/10.1016/j.chemosphere.2018.09.033

[8] Y. Ai, Y. Liu, W. Lan, J. Jin, J. Xing, Y. Zou, C. Zhao, X. Wang, The effect of pH on the U (VI) sorption on graphene oxide (GO): a theoretical study, Chem. Eng. J., 343 (2018) 460-466. http://dx.doi.org/10.1016/j.cej.2018.03.027

[9] L. Guo, Y. Xu, M. Zhuo, L. Liu, Q. Xu, L. Wang, C. Shi, B. Ye, X. Fan, W. Chen, Highly efficient removal of Gd (III) using hybrid hydrosols of carbon nanotubes/graphene oxide in dialysis bags and synergistic enhancement effect, Chem. Eng. J., 348 (2018) 535-545. https://doi.org/10.1016/j.cej.2018.04.212

[10] Y. Yang, Y. Yu, N.-n. Yang, B. Huang, Y.-f. Kuang, Y.-w. Liao, Adsorption behavior of isocyanate/ethylenediaminetetraacetic acid-functionalized graphene oxides for Cu^{2+} removal, Water Sci. Technol., 78 (2018) 2459-2468. https://doi.org/10.2166/wst.2018.520

[11] J. Zhang, M.S. Azam, C. Shi, J. Huang, B. Yan, Q. Liu, H. Zeng, Poly (acrylic acid) functionalized magnetic graphene oxide nanocomposite for removal of methylene blue, RSC Advances, 5 (2015) 32272-32282. https://doi.org/10.1039/C5RA01815C

[12] L. Yang, Z. Li, G. Nie, Z. Zhang, X. Lu, C. Wang, Fabrication of poly (o-phenylenediamine)/reduced graphene oxide composite nanosheets via microwave heating and their effective adsorption of lead ions, Appl. Surf. Sci., 307 (2014) 601-607. https://doi.org/10.1016/j.apsusc.2014.04.083

[13] A.A. Mizhir, A.A. Abdulwahid, H.S. Al-Lami, Chemical functionalization graphene oxide for the adsorption behavior of Bismarck Brown dye from aqueous solutions, Egyp. J. Chem., 63(5) (2020) 1676-1696. https://dx.doi.org/10.21608/ejchem.2020.21260.2271

[14] L. Li, C. Luo, X. Li, H. Duan, X. Wang, Preparation of magnetic ionic liquid/chitosan/graphene oxide composite and application for water treatment, Int. J. Biol. Macromol., 66 (2014) 172-178. https://doi.org/10.1016/j.ijbiomac.2014.02.031

[15] D. Depan, B. Girase, J. Shah, R. Misra, Structure–process–property relationship of the polar graphene oxide-mediated cellular response and stimulated growth of osteoblasts on hybrid chitosan network structure nanocomposite scaffolds, Acta Biomater., 7 (2011) 3432-3445. https://doi.org/10.1016/j.actbio.2011.05.019

[16] L. Cui, Y. Wang, L. Gao, L. Hu, L. Yan, Q. Wei, B. Du, EDTA functionalized magnetic graphene oxide for removal of Pb (II), Hg (II) and Cu (II) in water treatment: Adsorption mechanism and separation property, Chem. Eng. J., 281 (2015) 1-10. https://doi.org/10.1016/j.cej.2015.06.043

[17] R.W. Sabnis, Handbook of biological dyes and stains: synthesis and industrial applications, John Wiley & Sons 2010. https://doi.org/10.1002/9780470586242

[18] M.T. Sultan, H.S. Al-Lami, A.H. Al-Dujiali, Synthesis and characterization of alumina-grafted acrylic acid monomer and polymer and its adsorption of phenol and p-chlorophenol, Desalin.Water Treat., 150 (2019) 192–203. https://doi.org/10.5004/dwt.2019.23593

[19] T.J.M. Fraga, Z.S.B. de Souza, D.M.d.S.M. Fraga, M.N. Carvalho, E.M.P. de Luna Freire, M.G. Ghislandi, M.A. da Motta Sobrinho, Comparative approach towards the adsorption of Reactive Black 5 and methylene blue by n-layer graphene oxide and its amino-functionalized derivative, Adsorption, 26 (2020) 283-301. https//doi.org/doi:10.1007/s10450-019-00156-9

[20] E.S. Al-Allaq, H.S. Al-Lami, A.H. Al-Mowali, Synthesis and adsorption study of some chitosan acidic derivatives as dispersants for ceramic alumina powders, Egypt. J. Chem., 63(7), (2020) 2717-2736. https://dx.doi.org/10.21608/ejchem.2019.15492.1940

[21] M. Hasanzadeh, A. Simchi, H.S. Far, Nanoporous composites of activated carbon-metal organic frameworks for organic dye adsorption: Synthesis, adsorption mechanism and kinetics studies, J. Ind. Eng. Chem., 81 (2020) 405-414. https://doi.org/10.1016/j.jiec.2019.09.031

[22] C. Karthik, N. Swathi, D. Caroline, Green synthesized rGO-AgNP hybrid nanocomposite–An effective antibacterial adsorbent for photocatalytic removal of DB-14 dye from aqueous solution, J. of Environ. Chem. Eng., 8 (2020) 103577.
http://dx.doi.org/10.1016/j.jece.2019.103577

[23] M.T. Sultan, H.S. Al-Lami, A.H. Al-Dujiali, Synthesis and characterization of alumina-grafted acrylic acid monomer and polymer and its adsorption of phenol and p-chlorophenol, Desal. Water Treat., 150 (2019) 192-203. http://dx.doi.org/10.5004/dwt.2019.23593

[24] G. Wang, Z. Zhang, W. Li, C. Du, T. Chen, Production and characterization of modified biochar by corn cob and its ability to absorb phenol, IOP Conference Series: Materials Science and Engineering, IOP Publishing, 2020, pp. 012070. http://dx.doi.org/10.1088/1757-899X/729/1/012070

[25] H.T. Xing, J.H. Chen, X. Sun, Y.H. Huang, Z.B. Su, S.R. Hu, W. Weng, S.X. Li, H.X. Guo, W.B. Wu, NH_2-rich polymer/graphene oxide used as a novel adsorbent for removal of Cu (II) from aqueous solution, Chem. Eng. J., 263 (2015) 280-289.
https://www.cheric.org/research/tech/periodicals/doi.php?art_seq=1304278

[26] T. Manimekalai, G. Tamilarasan, N. Sivakumar, S. Periyasamy, Kinetic, equilibrium and thermodynamic studies of synthetic dye removal using plastic waste activated carbon prepared by CO_2 activation, Int. J. Chemtech. Res, 8 (2015) 225-240.

https://www.cabdirect.org/cabdirect/abstract/20153338805

[27] L. Wang, C. Shi, L. Pan, X. Zhang, J.-J. Zou, Rational design, synthesis, adsorption principles and applications of metal oxide adsorbents: A Review, Nanoscale, 12 (2020) 4790-4815. https://doi.org/10.1039/C9NR09274A

[28] J. Bu, L. Yuan, N. Zhang, D. Liu, Y. Meng, X. Peng, High-efficiency adsorption of methylene blue dye from wastewater by a thiosemicarbazide functionalized graphene oxide composite, Diam. Relat. Mater., 101 (2020) 107604. http://doi.org/10.1016/j.diamond.2019.107604

[29] S.M.R. Goddeti, M. Bhaumik, A. Maity, S.S. Ray, Removal of Congo red from aqueous solution by adsorption using gum ghatti and acrylamide graft copolymer coated with zero-valent iron, Int. J. Biol. Macromol., 149 (2020) 21-30. https://doi.org/10.1016/j.ijbiomac.2020.01.099

[30] J. Xiao, L. Wang, J. Ran, J. Zhao, M. Tao, W. Zhang, Highly selective removal of cationic dyes from water by acid-base regulated anionic functionalized polyacrylonitrile fiber: Fast adsorption, low detection limit, reusability, React. Funct. Polym., 146 (2020) 104394. http://doi.org/10.1016/j.reactfunctpolym.2019.104394

[31] A.A. Mizhir, A.A. Abdulwahid, H.S. Al-Lami, Adsorption of carcinogenic dye Congo red onto prepared graphene oxide-based composites, Desal. Water Treat., 202 (2020) 381–395. http://doi: 10.5004/dwt.2020.26141

[32] J. Ma, P. Cai, W. Qi, D. Kong, H. Wang, The layer-by-layer assembly of polyelectrolyte functionalized graphene sheets: a potential tool for biosensing, Colloids Surf., A: Physico. Eng. Asp., 426 (2013) 6-11. https://doi.org/10.1016/j.colsurfa.2013.02.039

[33] L. Zhang, H. Luo, P. Liu, W. Fang, J. Geng, A novel modified graphene oxide/chitosan composite used as an adsorbent for Cr (VI) in aqueous solutions, Int. J. Biol. Macromol., 87 (2016) 586-596. https://doi.org/10.1016/j.ijbiomac.2016.03.027

[34] H. Ge, Z. Ma, Microwave preparation of triethylenetetramine modified graphene oxide/chitosan composite for adsorption of Cr (VI), Carbohydr. Polym., 131 (2015) 280-287. https://doi.org/10.1016/j.carbpol.2015.06.025

[35] L. Liu, C. Li, C. Bao, Q. Jia, P. Xiao, X. Liu, Q. Zhanc, Preparation and characterization of chitosan, Talanta, 93 (2012) 350-357. https://doi.org/10.1016/j.talanta.2012.02.051

[36] C. Zhao, L. Ma, J. You, F. Qu, R.D. Priestley, EDTA-and amine-functionalized graphene oxide as sorbents for Ni (II) removal, Desal. Water Treat., 57 (2016) 8942-8951. https://doi.org/10.1080/19443994.2015.1025438

[37] R. Jain, M. Shrivastava, Adsorptive studies of hazardous dye Tropaeoline 000 from an aqueous phase onto coconut husk, J. Hazard. Mater., 158 (2008) 549-556. https://doi.org/10.1016/j.jhazmat.2008.01.101

[38] S. Mishra, D. Mohapatra, D. Mishra, P. Chattopadhyay, G.R. Chaudhury, R. Das, Arsenic adsorption on natural minerals, J. Mater. Env. Sci., 5 (2014) 350-359. https://www.jmaterenvironsci.com/Document/vol5/vol5_N2/41-JMES-455-2013-Mishra.pdf

[39] B. Royer, N.F. Cardoso, E.C. Lima, J.C. Vaghetti, N.M. Simon, T. Calvete, R.C. Veses, Applications of Brazilian pine-fruit shell in natural and carbonized forms as adsorbents to removal of methylene blue from aqueous solutions—Kinetic and equilibrium study, J. Hazard. Mater., 164 (2009) 1213-1222. https://doi.org/10.1016/j.jhazmat.2008.09.028

[40] M. Islam, P.C. Mishra, R. Patel, Fluoride adsorption from aqueous solution by a hybrid thorium phosphate composite, Chem. Eng. J., 166 (2011) 978-985. https://doi.org/10.1016/j.cej.2010.11.087

[41] M.J. Rupa, A. Pal, B.B. Saha, Activated carbon-graphene nanoplatelets based green cooling system: Adsorption kinetics, heat of adsorption, and thermodynamic performance, Energy, 193 (2020) 116774. https://doi.org/10.1016/j.energy.2019.116774

[42] S. Ren, Z. Meng, X. Sun, H. Lu, M. Zhang, A.H. Lahori, S. Bu, Comparison of Cd^{2+} adsorption onto amphoteric, amphoteric-cationic and amphoteric-anionic modified magnetic bentonites, Chemosphere, 239 (2020) 124840. http://dx.doi.org/10.1016/j.chemosphere.2019.124840

[43] H.N. Tran, F. Tomul, H.T.H. Nguyen, D.T. Nguyen, E.C. Lima, G.T. Le, C.-T. Chang, V. Masindi, S.H. Woo, Innovative spherical biochar for pharmaceutical removal from water: Insight into adsorption mechanism, J. Hazard. Mater., (2020) 122255. https://doi.org/10.1016/j.jhazmat.2020.122255

[44] L. Alcaraz, I. García-Díaz, F.J. Alguacil, F.A. Lopez, Removal of Copper Ions from Wastewater by Adsorption onto a Green Adsorbent from Winemaking Wastes, BioResources, 15 (2020) 1112-1133. https://doi.org/10.15376/biores.15.1.1112-1133

إمتزاز صبغة بسمارك البنية الخطرة على أكسيد الكرافين ومشتقيه من الكيتوسان وثنائي أثيلين ثنائي أمين رباعي الحامض

[1]علاء عادل مزهر [2]هادي سلمان اللامي [2]علي عبدالرزاق عبدالواحد

[1]قسم علوم البحار التطبيقية، كلية علوم البحار، جامعة البصرة، البصرة-العراق

[2]قسم الكيمياء، كلية العلوم، جامعة البصرة، البصرة-العراق

المستخلص

تستند هذه الدراسة على تطوير المواد الممتزة البوليمرية لإزالة صبغة بسمارك براون السامة. تم استخدام طريقة هامر بتحويرات بسيطة للحصول على أوكسيد الكرافين GO من الجرافيت. أما المشتقان الآخران فقد تم تحضيرهما عن طريق تطعيم GO بالكيتوسان (GO/CS) ومن ثم بثنائي أثيلين ثنائي أمين رباعي الحامض (GO/CS/EDTA). تم مطيافية الأشعة تحت الحمراء (FTIR) لتحليل بنيتها الكيميائية. أجريت دراسات دفعية للتحقيق في أنظمة الامتزاز من GO ومشتقاتها ضد صبغة بسمارك براون السامة ، وأظهرت رد فعل جيد على الامتزاز من محاليلهم المائية. بدأ التحسين من أنظمة الامتزاز مع دراسة لتأثير الدالة الحامضية لمحلول الصبغة. وأظهرت النتائج أن القيم المثلى لدرجة الحموضة تختلف باختلاف نوع المواد المازة. ووجد أن ووجد ان قيم الدالة الحامضية، 3 و3 و5 كانت الأفضل لامتزاز صبغة بسمارك على GO، GO/CS، و GO/CS/EDTA، على التوالي، مع وقت إثارة يصل إلى 45 دقيقة. تم تحديد أيزوثيرم الامتزاز باستخدام لانكمير وفروندليش. حيث وجد أن نموذج لانكمير أكثر ملاءمة للنتائج التجريبية لامتزاز صبغة بسمارك على المواد المازة المحضرة. ووفقا للدراسات الحركية، وجد أن نموذج الدرجة الثانية الزائفة يناسب البيانات التجريبية أفضل من نموذج الدرجة الأولى الزائفة، وان عملية الأمتزاز عملية أنية وفقا للخصائص الديناميكية الحرارية ومن النوع الماص للحرارة.